

Stipica Novoselac

PhD Student
Josip Juraj Strossmayer University of Osijek
Mechanical Engineering Faculty in
Slavonski Brod
Croatia

Dražan Kozak

Full Professor
Josip Juraj Strossmayer University of Osijek
Mechanical Engineering Faculty in
Slavonski Brod
Croatia

Todor Ergić

Full Professor
Josip Juraj Strossmayer University of Osijek
Mechanical Engineering Faculty in
Slavonski Brod
Croatia

Darko Damjanović

Research Assistant
Josip Juraj Strossmayer University of Osijek
Mechanical Engineering Faculty in
Slavonski Brod
Croatia

Fatigue of Shaft Flange Bolted Joints Under Preload Force and Dynamic Response

The bolted joints are used for flange connections which are subjected to preload forces and dynamic loads. This combination of static and dynamic loads in threaded joints result with complex interaction of high mean stresses, high notch effect, thread flanks contact forces and moments, and contact surfaces slippage which leads to fatigue damage. The Multi-body system dynamic model of shaft was used for assessment of dynamic behavior. Finite element model of shaft flange connection, with detailed thread joints made of heat treatable steel 30CrNiMo8 under preload condition and nonlinear thread flanks contact, was created. The Rainflow cycle counting was used as a cycle count method for describing the load cycle with local stress-strain hysteresis loop. Influences of mean stresses, bolt diameter, and stress gradients were taken into account according to FKM guidelines. The most critical fatigue locations were obtained at thread roots.

Keywords thread fatigue, joint integrity, flange bolted joint, thread flanks contact, thread forces and moments, FKM guidelines, multiaxial fatigue.

1. INTRODUCTION

The bolted joints are most common connection type for flange connections in industry. These joints are subjected to preload forces due to the bolts tightening and dynamics loadings from operating conditions in-service. The bolted joints are critical points in oil and gas industry [1-3], automotive [4], and biomechanics [5, 6]. On one hand, the high-strength materials for bolts are used, because they have higher tensile and yield strength as well as cyclic properties. On the other hand, hydrogen embrittlement (HE) and stress corrosion cracking (SCC) are additional problem for high strength steels and their resistance decreases with the strength increase. Therefore, high strength steel materials for bolts are very prone to HE. In general, steels with yield strength below 800 MPa are resistant to HE [7, 8]. From this fact, it became evident that bolt strength class 10.9 and higher are critical points with regard to the HE. In addition, notch sensitivity usually linearly increases with material tensile strength. Fatigue analyses of threaded joints are mainly done on a basis of the nominal stresses with standards Eurocode 3 [9] and VDI 2230 guidelines [10]. For the offshore industry bolted joints are designed according to the ASME B16.5 [11] and API 6A: Specifications for Wellhead and Christmas Tree Equipment [12]. Recently, two standards for bolted joints requirements were published. ASME updated the 2010 PCC-1 "Guidelines for Pressure Boundary Bolted Flange Joint Assembly" with an appendix defining the requirements for training and qualification of

technicians working in the field of bolted joints. The European Committee for Standardization (CEN) re-published EN1591 Part 4 "Flanges and their Joints - Part 4: Qualification of personnel competency in assembly of the bolted connections of critical service pressurized systems". Nowadays, bolting technicians need to have the similar competence standards as welders. It is evident that industry in the future will have very high demand on reliability and integrity of bolted joints or any other threaded joints in general.

Nominal approaches does not consider local stress-strain state at the thread roots. Furthermore, nominal stress is very simple at first sight, because it is average stress in bolt cross-section. In engineering practice, problems arise due to details and influence factors which are not taken into account with nominal approach. The fatigue strength of a bolted joint depend on notch effect which contains both stress concentration and strength reduction by notches.

Local strain approach for threaded joints was recently published [13]. Forces and moments in threaded region is not uniformly distributed and the first engaged thread is subjected to highest load [14]. Failure analysis of threaded connections in large-scale tie rods with metric and trapezoidal threaded connection was recently published [15].

According to Croccolo et al. [16] it is difficult to find systematic and effective experiments about fatigue tests performed on screws or bolts. For investigation of bolted joints fatigue behaviour, multiaxial fatigue criterion is required [17]. The stress based critical plane approach is mainly used for estimation of multiaxial fatigue behaviour in high-cycle fatigue (HCF) regime. Besides stress based algorithm, energy quantities based on the critical plane approach are also used [17 - 19].

Critical plane approach theory takes as a starting point that the fatigue damage reaches its maximum

Received: May 2014, Accepted: August 2014

Correspondence to: Dražan Kozak

Josip Juraj Strossmayer University of Osijek,
Mechanical Engineering Faculty in Slavonski Brod, Croatia
E-mail: jdkozak@sfsb.hr

doi:10.5937/fmet1404269N

© Faculty of Mechanical Engineering, Belgrade. All rights reserved

FME Transactions (2014) 42, 269-276 269

value on the plane of maximum shear stress amplitude (τ_A), and the maximum normal stress (σ_{nmax}) relative to the plane with maximum τ_A is used to evaluate the detrimental effect of non-zero mean normal stress [20, 21]. According to the critical plane approach theory, fatigue damage depends on both τ_A and σ_{nmax} . Detailed investigation with local approach of stress gradients influence on bolted joint fatigue behavior was recently published [22].

In the present study, the fatigue analysis of flange bolted joints which are subjected to preload forces and dynamic response was performed. This combination of static preload forces and dynamic response create complex interaction of high mean stresses, high notch effects, and nonlinear contact interactions with slippage of thread flanks. This in turn lead to fatigue damage. Multi-body system (MBS) dynamic results of shaft were used for dynamic loadings. Finite element (FE) model of shaft flange connection, with detailed thread joints made of heat treatable steel 30CrNiMo8 was analyzed for fatigue. Rainflow cycle counting was used as cycle count method for describing the load cycle with local stress-strain hysteresis loop. Influences of mean stresses, bolt diameter, and stress gradients were taken into account according to the FKM guidelines.

2. MODELING

The first modeling phase included FE model of shaft with flange for MBS dynamic analysis. For dynamic analysis, coarse FE mesh was created with bolts modeled as beam elements. FE model is shown in Fig. 1. The bolt modeling approach with beam elements can be clearly seen in Fig. 1. Mesh was created with solid tetrahedral elements (Abaqus C3D10 elements) and beam elements (Abaqus B31 elements). The Model consists of 17330 solid and 16 beam elements. Total number of nodes is 27871. Beam elements are connected via the kinematic couplings between flange connection. However, dynamic analysis is not a target of this investigation. Therefore, only details regarding the fatigue will be briefly explained.

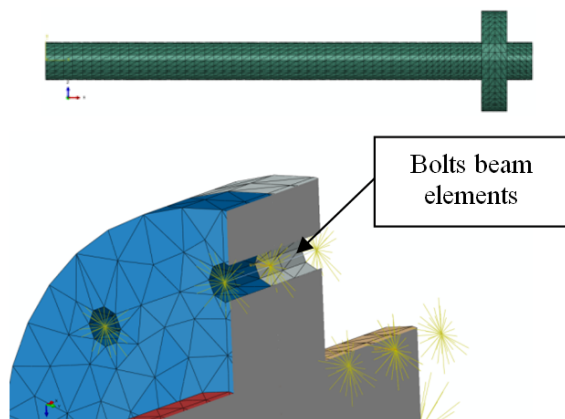


Figure 1. Coarse FE model for dynamic analysis

For fatigue analysis, which is a main target of this investigation, bolts and nuts mesh was created very fine with solid hexahedral elements (Abaqus C3D8 elements), as shown in Fig. 3. Additionally, flanges were also meshed finer than in the dynamic analysis with

tetrahedral elements with improved surface stress (Abaqus C3D10I elements) for achieving accurate stress results on contact surfaces with nuts and bolt heads. The number of C3D8 elements is 703448 and 42612 of elements type C3D10I. The total number of nodes is 853838. Thread profile was defined as axi-symmetric because it has been found that helical effect does not influence the load distribution [23]. Nonlinear contacts were modeled with sliding surface contact. Contact surfaces are shown in Fig. 4. According to the VDI 2230 Guidelines in the case of uncertainty about friction in the thread flanks and under the bolt head and nut, the lowest possible coefficient of friction must be selected [24]. For steel – steel combination in dry state, $\mu = 0.1 - 0.23$ [24]. Therefore, friction coefficient was set to $\mu = 0.1$, as the lowest possible. The flange bolted joints consist of M10 bolts, strength class 12.9 with metric standard thread (pitch according to DIN 13-1 and -28, stress cross section and cross section at minor diameter according to DIN 13-28, and minimum yield point according to DIN EN ISO 898-1).

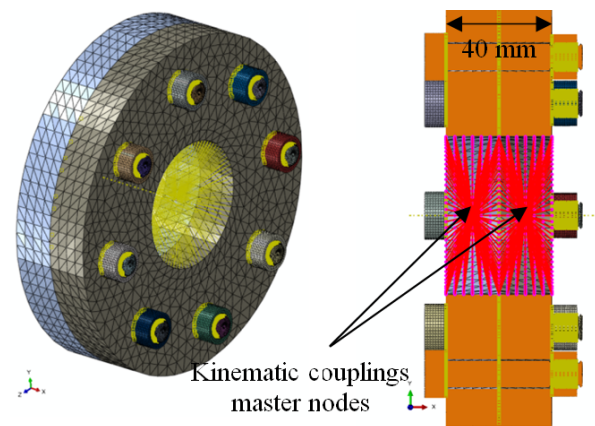


Figure 2. Fine FE model for fatigue analysis

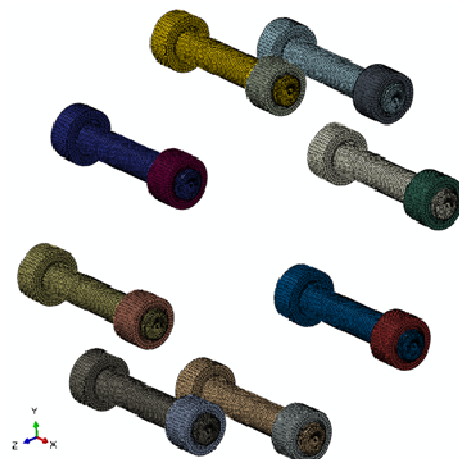


Figure 3. Bolts and nuts mesh with solid hexahedral elements for fatigue analysis

During the in-service life of flange bolted joints, first load is due to the tightening. Bolts preload force (F_p) was defined according to force at yield point ($F_{0.2}$) for M10 bolt, strength class 12.9, with value of $F_{0.2} = 64000$ N [24]. Applied preload force was $F_p = 44800$ N. This value corresponds as 70% of $F_{0.2}$. Abaqus command „Bolt Preload“ was used for application of the forces on

surface in middle of each bolt shank. The tightening of all bolts was simultaneously introduced in first step of FE analysis. Further steps were defined with results from dynamic analysis which contains displacements and rotations of kinematic coupling master nodes. These displacements and rotations of master nodes are used for loadings of fine model for fatigue analysis, as shown in Fig. 5. Duration of loading is 1.5 s.

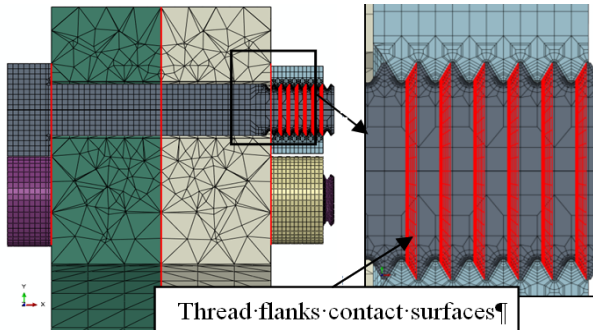


Figure 4. Contact surfaces

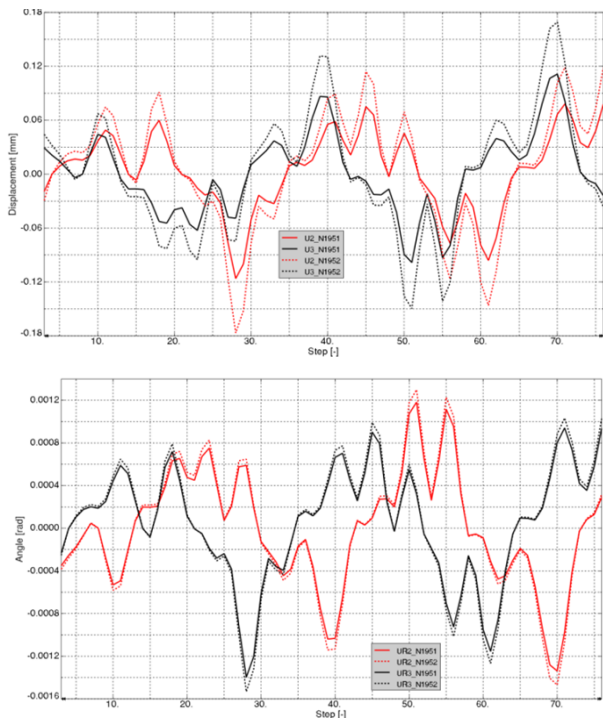


Figure 5. Displacements and rotations of kinematic couplings master nodes

30CrNiMo8 steel monotonic and cyclic properties are shown in Table 1.

Table 1. Material cyclic and monotonic properties

Property	Value
Modulus of elasticity, E [MPa]	212000
Poisson coefficient, ν [-]	0.3
Tensile strength, R_m [MPa]	1250
Yield strength, $R_{0.2}$ [MPa]	1050
Cyclic coefficient of hardening, K' [MPa]	2012.5
Cyclic exponent of hardening, n' [-]	0.15
Elongation at fracture, A [%]	9.3

Material properties are defined according to the DIN EN 10 083-1 for quenched and tempered condition. Smooth circular specimen diameter is 7.5 mm. $S-N$ curve for alternating tension/compression loading

(stress ratio $R = -1$) and relative stress gradient ($\chi' = 0$) with survival probability defined at 97.5% is shown in Fig. 6. The fatigue limit for $R = -1$ have a knee-point in the $S-N$ curve at $2 \cdot 10^6$ cycles with the slope of $k = 12$. Alternating fatigue strength under tension/compression ($R = -1$) is $\sigma_{D,tc} = 565$ MPa [25].

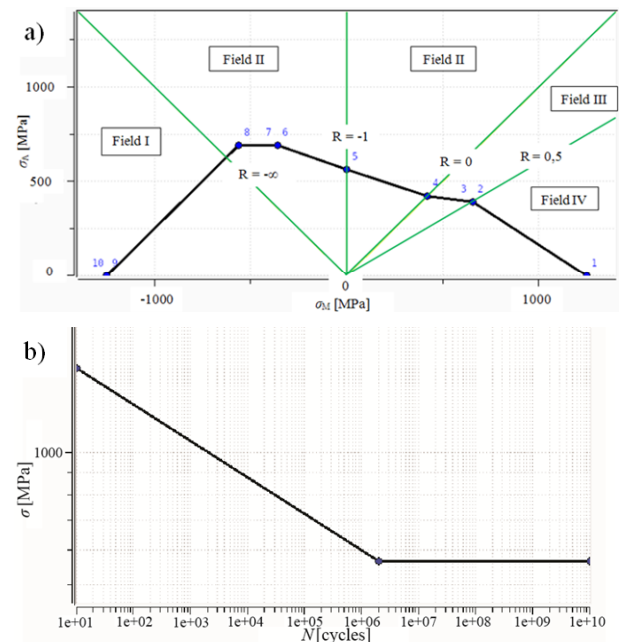


Figure 6. 30CrNiMo8 steel a) Haigh diagram and b) $S-N$ curve for survival probability of 97.5%

FE analysis was done in Abaqus 6.12 (Simulia, Providence, RI, USA). The stress tensors with fatigue influence factors and nonlinear cyclic material properties were further calculated in the FemFat 5.0 (ECS, Steyr, Austria) software.

3. FATIGUE ANALYSIS

The fatigue calculation starts from known smooth specimen $S-N$ curve and Haigh diagram with stress tensors from FE analysis. Furthermore, multiaxial interaction between stress amplitude tensors and mean stress tensors was solved with critical plane approach in combination with the Haigh diagram. Each node with particular local $S-N$ curve at bolts is calculated from the specimen cyclic properties and fatigue influence factors, such as notch effects, diameter, mean stress, mean stress rearrangement due to local plastification, and statistics (range of dispersion and survival probability). These all influences are taken into account at a locally modified $S-N$ curve and Haigh diagram to obtain correct fatigue limit at critical areas, because material cyclic properties are valid for the smooth cylindrical specimen, not notched structure. If in the loading spectrum of a flange bolted joints local stress values are in the elasto-plastic area of material, than mean stress tensors are rearranged by the means of Neuber-hyperbola rule in the cycle stabilised stress-strain curve. This means that the unrealistic high stress values due to the linear-elastic material definition in FE analysis and stress concentrations in notches will be rearranged to achieve realistic nonlinear cyclic material behaviour. Mean

stress rearrangement was done according to Neuber-hyperbola with FemFat PLAST. Haigh diagram was used to define the most critical cutting plane angle and the damaging factor for each node on bolted joints. The plane with maximum damage is assumed as the most critical for fatigue failure. Cutting plane was defined for every 10°. The relative stress gradients (χ') and mean stresses (σ_M) influences the slope (k), endurance cycle limit (N_D), and fatigue limit (σ_D) of local $S-N$ curve. Influence factors of size and statistics influences only fatigue limit. Results of fatigue safety factors (SF) against fatigue limit are for constant mean stress in Haigh diagram:

$$SF = \frac{\sigma_{Aall}}{\sigma_A} \quad (1)$$

where σ_{Aall} is the allowable stress amplitude and σ_A is the maximum stress amplitude during fatigue load spectrum.

The equivalent stress algorithm used for the multiaxial fatigue failure was scaled normal stress in critical plane which takes the damaging effect of shear into account and is recommended for ductile materials [26]. The algorithm for equivalent stress calculation makes reduction of the multiaxial stress state to the equivalent state with a criterion suitable for a ductile material, such as steel. From the obtained equivalent stress history in time domain, a Rainflow cycle counting is applied to identify closed cycles in the stress-strain-path. This means that the resultant loading is saved in a square 64x64 amplitude/mean stress matrix.

Influence of size was defined with the bolt diameter of 10 mm. It has been found that the fatigue life reduces as the bolt nominal size increases [27]. The size influence factor is determined in accordance with FKM-Guidelines [25]. The range of dispersion (T_S) is defined as the ratio of the bolt fatigue strength at survival probability of $P_S = 10\%$ to fatigue strength at $P_S = 90\%$. Recommended value for steel is 1.26 [26, 28]. This value is taken from experiments. Fatigue analysis was done with high survival probability of $P_S = 99\%$. The statistics applied regarding distribution type is the Gaussian Log-Normal distribution for the calculation of statistics influencing variables, both for range of dispersion and survival probability.

Fatigue limits under bending conditions are always higher than under the tension/compression. The gradient support effect was confirmed in research with tension/compression and bending fatigue experimental investigations [29, 30]. Gradient support effect is determined with the relative stress gradient (χ').

According to FKM-Guidelines [25], support factor can be calculated in dependence from relative stress gradient values:

for $\chi' \leq 0.1$ MPa/mm support factor n can be calculated:

$$n = 1 + \chi' \cdot 10^{-\left(a_G - 0.5 + \frac{R_m}{b_G}\right)} \quad (2)$$

for $0.1 \text{ MPa/mm} < \chi' \leq 1 \text{ MPa/mm}$ support factor n is:

$$n = 1 + \sqrt{\chi'} \cdot 10^{-\left(a_G + \frac{R_m}{b_G}\right)} \quad (3)$$

for $1 \text{ MPa/mm} < \chi' \leq 100 \text{ MPa/mm}$ support factor n is:

$$n = 1 + \sqrt[4]{\chi'} \cdot 10^{-\left(a_G + \frac{R_m}{b_G}\right)} \quad (4)$$

where a_G and b_G are constants and for the steels are 0.5 and 2700, respectively [25].

According to the FKM-Guidelines [25], mean stress influence is taken into account with mean stress factor ($K_{AK,\sigma}$), which depends on the type of overloading. It describes the way how the stress may increase in the case of a possible overload in-service. Selected type Fl is when the mean stress (σ_M) remains the same. Fields of mean stresses for calculation of the $K_{AK,\sigma}$ are separated in four fields. These fields depend on the stress ratio R or on the mean stress σ_M . All four fields are described below.

Field I: $R > 1$, field of fluctuating compression stress, where $R = +$ or $-\infty$ is the zero compression stress.

Field II: $-\infty \leq R \leq 0$, where $R < -1$ is the field of alternating compression stress. $R = -1$ is the completely reversed stress, while $R > -1$ is the field of alternating tension stress.

Field III: $0 < R < 0.5$, field of pulsating (or fluctuating) tension stress, where $R = 0$ is the zero tension stress.

Field IV: $R \geq 0.5$, field of high pulsating tension stress.

All four fields were marked in Fig. 6 in Haigh diagram. Calculation for the type of overloading Fl is according to the following equations.

Field I:

For $\sigma_{max} = \sigma_M / (K_{E\sigma} \cdot \sigma_{WK}) < -1 / (1 - M_\sigma)^2$ there is:

$$K_{AK,\sigma} = \frac{1}{1 - M_\sigma} \quad (5)$$

Field II:

For $-1 / (1 - M_\sigma) \leq \sigma_{max} \leq 1 / (1 + M_\sigma)$ there is:

$$K_{AK,\sigma} = 1 - M_\sigma \cdot \sigma_{max} \quad (6)$$

Field III:

For $1 / (1 + M_\sigma) < \sigma_{max} < 3 + M_\sigma / (1 + M_\sigma)^2$

$$K_{AK,\sigma} = \frac{1 + M_\sigma / 3}{1 + M_\sigma} - \frac{M_\sigma}{3} \cdot \sigma_{max} \quad (7)$$

Field IV:

For $\sigma_{max} \geq 3 + M_\sigma / (1 + M_\sigma)^2$ there is:

$$K_{AK,\sigma} = \frac{3 + M_\sigma}{3 \cdot (1 + M_\sigma)^2} \quad (8)$$

where σ_{max} is the maximum stress.

Mean stress sensitivity is calculated according to the following equations for normal and shear stress, respectively:

$$M_\sigma = a_M \cdot \left(\frac{R_m}{1000}\right) + b_M \quad (9)$$

$$M_{\tau} = f_{w\tau} \cdot M_{\sigma} \quad (10)$$

where a_M and b_M are material constants. For steel $a_M = 0.35$ and $b_M = -0.1$. $f_{w\tau}$ is shear fatigue strength factor.

4. RESULTS AND DISCUSSION

The stress tensors from FE analysis with bolts tightening step and further dynamic loadings were analyzed in time domain to obtain fatigue safety factors, stress amplitudes, mean stresses, relative stress gradients, stress ratios, and fatigue limit. The stress tensors were written only for bolts finite elements from threaded region and close to the bolt head. The reason for such approach was to have a reasonable amount of data and to analyze only most critical areas, because threaded joints are generally known for their high stress concentrations, high stress gradients, and fatigue failures. The Max Principal stress history for the most critical node at first engaged thread root is shown in Fig. 7. The most critical node is determined with fatigue analysis. Therefore, this node is of particular interest. The Max Principal stress distribution for step with maximal value is shown on cut view of bolt 6. It can be seen that high stress concentrations occur at first 3 thread roots. It can be also noticed that the stress values are very high. This is result of linear-elastic material definition and high notch effect at thread roots. These values prove the necessity for stress rearrangement by means of Neuber-hyperbola. Deformation scale for Max Principal stress distribution on bolt 6 is 25.

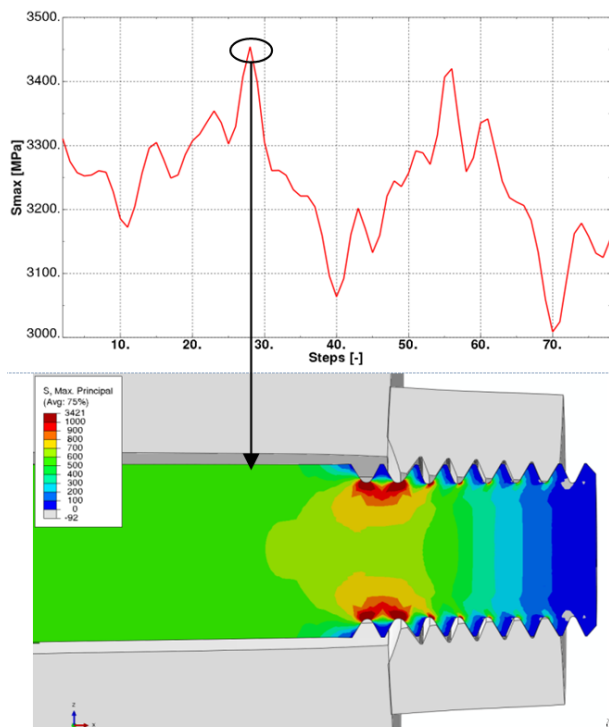


FIGURE 7. Max Principal stress history for most critical node on bolt 6

Magnitude of total force due to contact pressure and frictional stress (F_{CFTM}) is shown on diagram of Fig. 8. From diagram, maximal obtained value of $F_{CFTM} = 12351$ N. It can be noticed that the value of F_{CFTM} after tightening in first step has slightly decreased over the

steps with dynamic loadings. Magnitude of total moment due to contact pressure and frictional stress (M_{CMTM}) is shown on diagram of Fig. 9. From diagram, maximal obtained value of $M_{CMTM} = 877946$ N·mm.

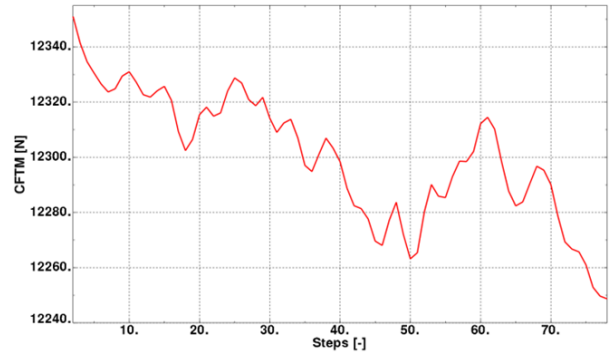


Figure 8. Magnitude of total force due to contact pressure and frictional stress

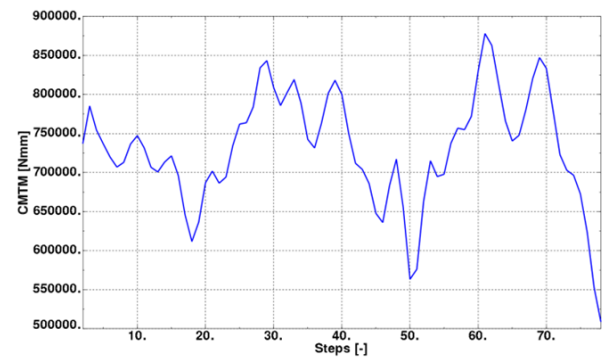


FIGURE 9. Magnitude of total moment due to contact pressure and frictional stress

Fatigue results of SF are shown in Fig. 10 for all bolts and $P_S = 99\%$. For each bolt, calculated minimal SF is placed next to bolt position. Bolt 6 has a lowest $SF_{min} = 1.39$.

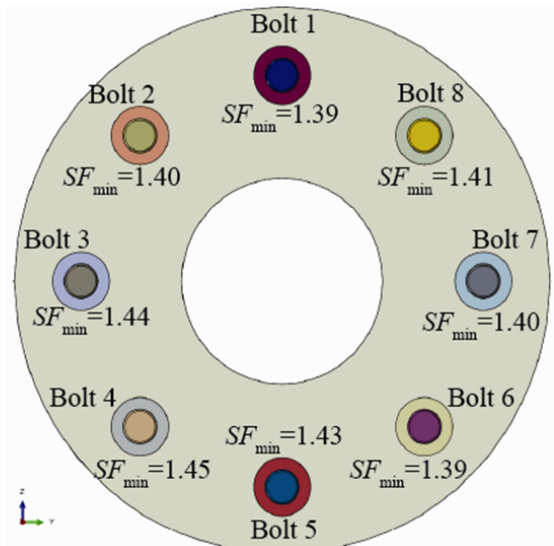


FIGURE 10. Fatigue safety factors

The stress amplitudes distribution on bolt 6 is shown in Fig. 11 a). The distribution clearly shows that the highest stress amplitudes occur at threaded region of bolt. Maximal value of $\sigma_A = 219$ MPa was obtained at first engaged thread root. It can be also noticed that at

the nominal section of bolt (i. e., at bolt shank) stress amplitudes are significantly lower. In middle part approximately $\sigma_A = 10$ MPa, whereas in area close to the bolt head $\sigma_A = 50$ MPa. The distribution of fatigue safety factors is shown in Fig. 11 b). The results show that the minimal safety factor occur at first engaged thread with value of $SF_{min} = 1.39$. Stress amplitude distribution and fatigue safety factors are shown in Fig. 12 a) and b), respectively with detailed 3D view on threaded region.

The results clearly show the difference in most critical region and nominal region from fatigue point of view. Relative stress gradient at node with SF_{min} : $\chi' = 8.4$ MPa/mm. However, on bolt shank $\chi' = 0.4$ MPa/mm. The most critical node in first engaged thread root have a mean stress $\sigma_M = 1016$ MPa, whereas at bolt shank $\sigma_M = 526$ MPa. Haigh diagrams for thread root node and bolt shank node are shown in Fig. 13 a) and b), respectively. From Haigh diagrams can be seen difference in stress amplitudes and mean stresses between thread root and nominal bolt shank. On Fig. 13 a) it is marked how the fatigue safety factor is measured with the case when mean stress remains the same. Furthermore, stress ratio of $R = 0.7$ was obtained for thread root, whereas node at bolt shank have $R = 0.9$. Regarding the fatigue limits at particular area, it is interesting to observe that thread root fatigue limit is $\sigma_D = 303$ MPa, whereas $\sigma_D = 413$ MPa for bolt shank. Lower fatigue limit at thread root is a result of high notch effect (stress concentration and stress gradients). The fatigue safety factor at bolt shank is $SF = 10.2$.

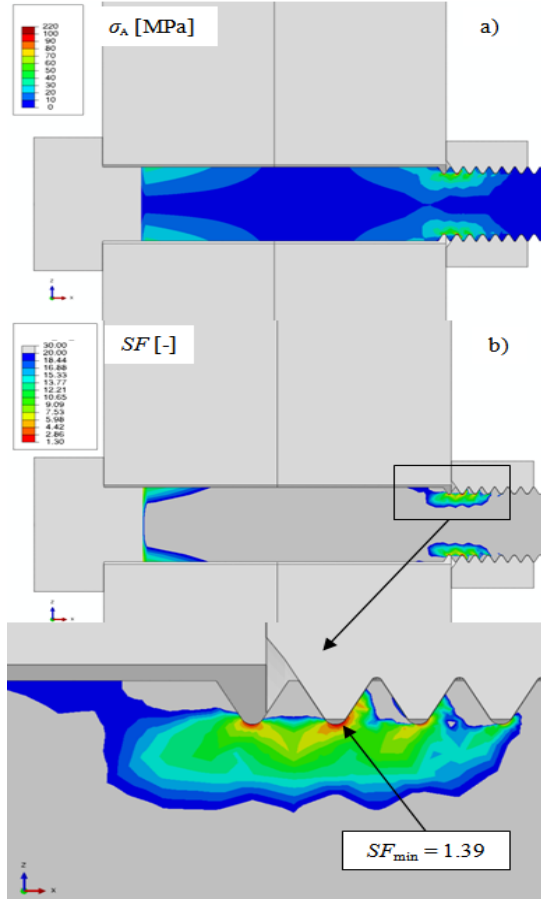


Figure 11. Fatigue results a) stress amplitudes and b) fatigue safety factors at most critical bolt

Fatigue safety factors corresponds to so-called knee point at local $S-N$ curve. In engineering standards and regulations, the $S-N$ curve knee point is defined as the transition to infinite life. The $S-N$ curve is generally limited to 10^6 , $2 \cdot 10^6$, $5 \cdot 10^6$, 10^7 cycles or some other value depending on the standard or structure (69). Recent experimental results up to giga-cycles (i. e., $1 \cdot 10^9$) shows that there is a further decline of the $S-N$ curve beyond the knee point at higher cycles. The fatigue strength decline of $\approx 10\%$ per decade is usually assumed for engineering practice. Fatigue limit is usually given by the average alternating stress σ_D and the certain survival probability.

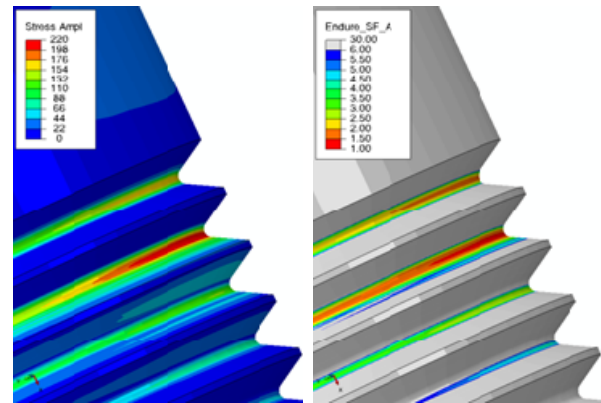


Figure 12. Fatigue results a) stress amplitudes and b) fatigue safety factors over threaded region at bolt 6

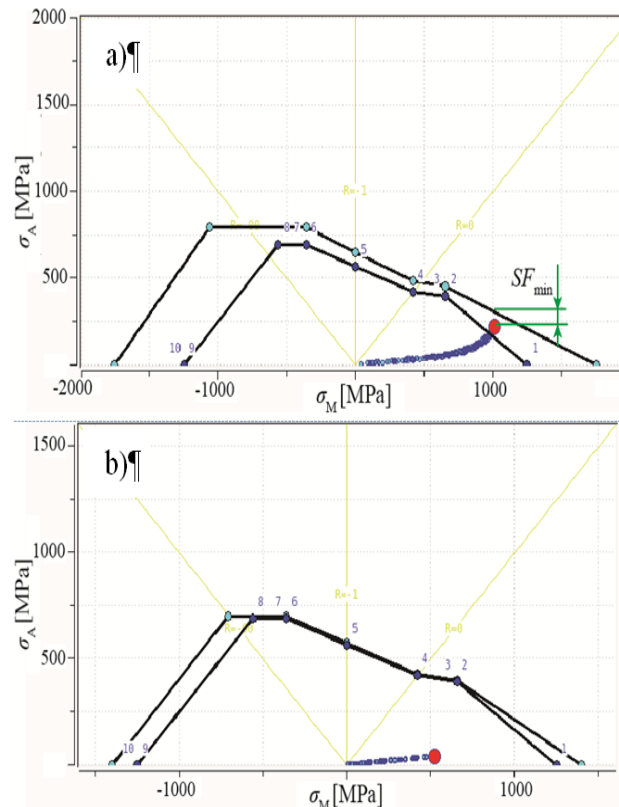


FIGURE 13. Haigh diagrams for node at a) first engaged thread root and b) bolt shank.

The further drop of fatigue strength in the high-cycle range can be considered using $S-N$ curve with fictitious slopes beyond the knee point of $k' = 2k - 1$ or $2k - 2$ (according to Haibach (56)) depending on material condition (wrought, cast or welded). Various standards

and regulations point out (58, 26, 70) that the fatigue limit does not exist in the case of jointed components such as press-fits or bolted joints because of fretting, high temperatures, and/or corrosion (71). Therefore, fatigue safety factors and reliability for higher number of cycles should be done with fatigue „limit“ corresponding to that higher number of cycles. For instance, to determine the fatigue safety factors of threaded joint for $2 \cdot 10^7$ cycles, they should be calculated with decreased fatigue limit value beyond knee point.

5. CONCLUSIONS

Under the parameters of dynamic analysis, FE, and fatigue analysis with influence factors of this study, the following conclusions were drawn concerning the fatigue of flange bolted joints for survival probability of $P_S = 99\%$:

- From fatigue results, the most critical fatigue locations were obtained at thread roots,
- Thread roots are exposed to high notch effect with maximum stress amplitude of $\sigma_A = 219$ MPa and relative stress gradient of $\chi' = 8.4$ MPa/mm,
- Obtained local fatigue limit for bolts made of 30CrNiMo8 steel, strength class 12.9, is $\sigma_D = 303$ MPa. This local value is valid only at first engaged thread root with preload condition of 70% of force at yield point ($F_{0.2}$), stress ratio of $R = 0.7$, and $P_S = 99\%$,
- Bolt shank is exposed to much lower stress amplitudes and notch effect.

ACKNOWLEDGMENT

The authors would like to thank AVL company for usage of Abaqus and FemFat softwares.

REFERENCES

- [1] Esaklul, K.A., Ahmed, T.M.: Prevention of failures of high strength fasteners in use in offshore and subsea applications, *Eng. Fail. Anal.*, Vol. 16, No. 3, pp. 1195–1202, 2009.
- [2] Sungkon, H.: Fatigue analysis of drillstring threaded connections, in: *Proceedings of The Thirteenth International Offshore and Polar Engineering Conference*, 25–30.05.2003, Hawaii, USA, pp. 202–208.
- [3] Shahani, A.R., Sharifi, S.M.H.: Contact stress analysis and calculation of stress concentration factors at the tool joint of a drill pipe, *Mater. Design*, Vol. 30, No. 9, pp. 3615–3621, 2009.
- [4] Cho, S.S., Chang, H., Lee, K.W.: Dependence of fatigue limit of high-tension bolts on mean stress and ultimate tensile strength, *Int. J. Automot. Techn.*, Vol. 10, No. 4, pp. 475–479, 2009.
- [5] Novoselac, S., Ergić, T., Kozak, D., Sertić, J., Pacak, M., Influence of dental implant screw preload force on high-cycle fatigue (in Croatian), in: *Proceedings of 5th Croatian Society of Mechanics*, 06-07.06 2013, Croatia, pp. 137-142.
- [6] Novoselac, S., Ergić, T., Kozak, D., Baškarić, T., Structural durability of dental implants (in Croatian), in: *Proceedings of 6th Croatian Society of Mechanics*, 29-30.05.2014, Croatia, pp. 251-256.
- [7] McEvily, A. J.: *Atlas of Stress Corrosion and Corrosion Fatigue Curves*, ASM International, 1990.
- [8] Bickford, J.H.: *An introduction to the design and behavior of bolted joints*. 2nd Ed. Marcel Dekker, 1990.
- [9] Eurocode No. 3: Design of steel constructions, Part 1. Beuth-Verlag, Berlin; 1993.
- [10] Verein Deutscher Ingenieure, VDI 2230 Guidelines, 2003.
- [11] ASME/ANSI B16 – standards of pipes and fittings, 2003.
- [12] API Spec 6A, Specification for wellhead and christmas tree equipment. Washington DC, American Petroleum Institute, 1996.
- [13] Schneider, R., Wuttke, U., Berger, C.: Fatigue Analysis of Threaded Connections Using the Local Strain Approach, *Procedia Eng.*, Vol. 2, No. 1, pp. 2357–2366, 2010.
- [14] Patterson, E.A., Kenny, B.: A modification to the theory for the load distribution in conventional nuts and bolts, *J. Strain Anal. Eng. Des.*, Vol. 21, No. 1, pp.17–23, 1986.
- [15] Duan, W., Joshi, S.: Failure analysis of threaded connections in large-scale steel tie rods, *Eng. Fail. Anal.*, Vol. 18, No. 8, pp. 2008-2018, 2011.
- [16] Crococolo, D., Agostinis, M., Vincenzi, N.: A contribution to the selection and calculation of screws in high duty bolted joints, *Int. J. Press. Vessels Pip.*, Vol. 96-97, pp. 38–48, 2012.
- [17] Fares, Y., Chaussumier, M., Daidie, A., Guillot, J.: Determining the life cycle of bolts using a local approach and the Dang Van criterion, *Fatigue Fract. Engng. Mater. Struct.*, Vol. 29, No. 8, pp. 588–596, 2006.
- [18] Liao, R., Sun, Y., Liu, J., Zhang, W.: Applicability of Damage Models for Failure Analysis of Threaded Bolts, *Eng. Fract. Mech.*, Vol. 78, No. 3, pp. 514–524, 2011.
- [19] Susmel, L., Tovo, R.: Estimating fatigue damage under variable amplitude multiaxial fatigue loading, *Fatigue Fract. Engng. Mater. Struct.*, Vol. 34, No. 12, pp.1053–1077, 2011.
- [20] McDiarmid, D.L.: A shear stress based critical-plane criterion of multiaxial fatigue failure for design and life prediction, *Fatigue Fract. Eng. Mater. Struct.*, Vol. 17, No. 12, pp. 1475–1484, 1994.
- [21] Lazzarin, P., Susmel, L.: A stress-based method to predict lifetime under multiaxial fatigue loadings, *Fatigue Fract. Eng. Mater. Struct.*, Vol. 26, No. 12, pp. 1171–1187, 2003.
- [22] Novoselac, S., Kozak, D., Ergić, T., Šimić, I.: Influence of Stress Gradients on Bolted Joint

Fatigue Behaviour Under Different Preloads and Cyclic Loads Ratio. Structural Integrity and Life, Vol. 14, No. 1, pp. 3-16, 2014.

- [23] Chen, J.J., Shih, Y.S.: A study of the helical effect on the thread connection by three dimensional finite element analysis, Nucl. Eng. Des., Vol. 191, No. 2, pp. 109–116, 1999.
- [24] Verein Deutscher Ingenieure, VDI 2230 Guidelines, 2003.
- [25] Forschungskuratorium Maschinenbau (FKM). Analytical strength assessment of components in mechanical engineering, 5th Ed. VDMA Verlag GmbH, 2003.
- [26] ECS Steyr. FemFat 4.8: MAX Manual. St. Valentin, 2007.
- [27] Majzoobi, G.H., Farrahi, G.H., Habibi, N.: Experimental evaluation of the effect of thread pitch on fatigue life of bolts. Int. J. Fatigue, Vol. 27, No. 2, pp.189–196, 2005.
- [28] Haibach, E., Matschke, C.: Normierte Wöhlerlinien für ungekerbte und gekerbte Formelemente aus Baustahl, Stahl u. Eisen, Vol. 101, No. 3, pp. 21-27, 1981.
- [29] Papadopoulos, I. V., Panoskaltsis, V. P.: Invariant formulation of a gradient dependent multiaxial high-cycle fatigue criterion, Eng. Fract. Mech., Vol. 55, No. 4, pp. 513-528, 1996.
- [30] Morel, F., Morel, A., Nadot, Y.: Comparison between defects and micro-notches in multiaxial fatigue – The size effect and the gradient effect, Int. J. Fatigue, Vol. 31, No. 2, pp. 263-275, 2009.

ЗАМОР ВИЈЧАНОГ СПОЈА ПРИРУБНИЦЕ ВРАТИЛА ПОД ДЈЕЛОВАЊЕМ СИЛА ПРИТЕЗАЊА И ДИНАМИЧКОГ ОДЗИВА

Стипица Новоселац, Дражан Козак, Тодор Ергић,
Дарко Дамјановић

Вијчани спојеве кориштени за прирубничке спојеве подвргнути су силама притезања и динамичким оптерећењима. Наведена комбинација статичких и динамичких оптерећења у вијчаним спојевима резултира с комплексном интеракцијом високих средњих напрезања, високог ефекта зарезног дјеловања, сила и момената на боковима навоја и клизањем контактних површина што доводи до заморног оштећења. *Мулти-боду систем* динамички модел вратила кориштен је за одређивање динамичког понашања. Модел коначних елемената споја прирубнице вратила с детаљним навојним спојевима од топлински обрађеног челика 30ЦрНиМо8 креиран је за оптерећења услијед притезања вијака с нелинеарним контактима. *Раинфлов* бројање циклуса кориштено је за описивање циклуса оптерећења с локалном петљом хистерезе напрезања-деформација. Утјецаји средњих напрезања, промјера вијка и градијената напрезања узети су у обзир према ФКМ препорукама. Најкритичније локације с обзиром на замор добивене су у коријенима навоја.